Chapter 8

$CuInS_2/In_2S_3$ SOLAR CELL PREPARED USING CSP TECHNIQUE: DESIGN MODIFICATIONS FOR IMPROVED PERFORMANCE

8.1 Introduction

In the earlier chapter we described the details of preparation and characterization of $CuInS_2/In_2S_3$ solar cell. The speciality of our work was that we used CSP technique for the deposition of both absorber and buffer layers, as it is very convenient to dope or vary the stoichiometry of the semiconductor layer through this technique. Moreover, here the buffer layer was In_2S_3 which is a wide band gap material having no toxic element like cadmium.

The first difficulty, which we had to overcome in this work, was the sequence of deposition. We could not deposit $CuInS_2$ over In_2S_3 layer. Hence we could not prepare 'real' superstrate structure. Instead, we prepared the cell with structure ITO/$CuInS_2$/In_2S_3/electrode and illumination was given through $CuInS_2$ side. However measurements showed that there was enough intensity reaching the junction region for carrier generation. But much more difficulty was created by the diffusion of copper from $CuInS_2$ layer into In_2S_3 layer. This made the junction very much imperfect. Diffusion of copper from $CuInS_2$ led to the formation of Cu vacancies, making the layer highly resistive. It was quite clear that these changes affected junction barrier leading to considerable reduction in short circuit current and fill factor. Moreover the diode quality factor was rather high indicating high recombination loss.

In this chapter we describe in detail the modifications made in the design aspects of the cell, so as to minimize (if not avoid) the difficulties we have experienced in the functioning of the cell in the preliminary stages. Variations in the thickness and stoichiometry of absorber and buffer layers, and trying different materials for top electrode were the major changes and these modifications resulted in

large improvement of cell parameters. These modifications were selected based on our earlier studies done on these materials.

It is worth mentioning here that we did not try etching using KCN [1-3] to remove unwanted phases of copper or doping using Na [4]. We also did not give any antireflection coating to prevent loss due to reflection of light from cell surface.

8.2 Device Fabrication

As stated earlier, we tried variations in thickness of absorber and buffer layers of the cell. This was mainly to accommodate copper diffusion. When we increased thickness of In_2S_3 layer, we could get a layer of pure In_2S_3 layer over the Cu diffused region. Similarly when CIS layer thickness was increased we could get, in the lower region, a layer of CIS, having high Cu concentration. Usually the volume of solution sprayed for depositing $CuInS_2$ was 375 ml while for depositing In_2S_3 layer 200 ml solution was sprayed. Corresponding thickness of the absorber layer was 0.6 μm while that of buffer layer was 0.5 μm. In order to increase buffer layer thickness, considering the copper diffusion from the copper indium sulfide layer to indium sulfide layer, two layers of In_2S_3 were sprayed in two steps (by spraying first 200 ml and 150 ml later) so as to make the total buffer layer thickness ~ 0.85 μm. After spraying 200 ml, the cell was allowed to cool to room temperature. Then it was reheated to 300°C to spray the remaining 150 ml. This procedure was accepted to avoid formation of pinholes. After spraying 150 ml the cell was kept at the preparation temperature itself for half an hour. Similarly for increasing absorber layer thickness, two layers of $CuInS_2$ were deposited by spraying 375 ml first and 300 ml later, making absorber layer, 1.1 μm thick. Here, the cell was kept at the preparation temperature for 1 hour after deposition. If the whole solution were sprayed in a single stretch, it would have led to the formation of pinholes in the film. In the present work we prepared three sets of samples. The first one was having single layer absorber and buffer (named as Cell-A). The second one was having two layers of absorber (named

as Cell-B) and the third one was having two layers of buffer (named as Cell-C). These three cases will be discussed in the following sections.

Cu/In, S/Cu and In/S ratios of the films were controlled by varying the molar concentrations of respective solutions. In the case of $CuInS_2$ films, Cu/In ratio was kept at 1.2 and 1 while S/Cu ratio was kept at 5 in solution. While preparing In_2S_3 layer, In/S ratio was kept at 1.2/8 in the solution as it was showing maximum photosensitivity [5]. Top electrode was thin film of Al or Ag (~ 45 nm), which was deposited over the In_2S_3 layer using physical vapor deposition. In all the cases illumination was given through absorber side due to the nature of the electrode. Always incident intensity was 100 mW/cm^2 avoiding heating of the sample as described in section 7.3. We also measured transmitted intensity through In_2S_3 side for Cell A, B, and C and found that values are ~ 20 mW/cm^2 (Cell-A), ~10 mW/cm^2 (Cell- B and C) respectively. This proved that enough intensity was available at junction region for carrier generation.

8. 3 Results and Discussion

8.3.1 Cell-A

At first we deposited a single layer of $CuInS_2$ (by spraying 375 ml solution) and In_2S_3 (by spraying 200 ml solution). Here Cu/In ratio for $CuInS_2$ was kept at 1 in the solution. The films were slightly copper deficient (Cu/In=0.7) as observed from EDAX measurements. This avoided formation of Cu_xS, $CuIn_5S_8$ or introduction of Cu_{In} antisite defects [1]. Moreover, no such phases were identified from the structural (XRD) and stoichiometric (XPS) analysis. Again Cu rich films may give rise to leakage current through electron tunneling at the junction. Thus we could avoid the toxic KCN etching before fabricating the cell. We also observed that photosensitivity of $CuInS_2$ film increased on decreasing the Cu/In ratio.

A thin layer of indium (50 Å) was evaporated onto the top of the cell followed by annealing at 100°C for 30 minutes. Aluminium (Al) was deposited over this, using

physical vapor deposition, as the top electrode. Diffusion of indium might be reducing the sheet resistance of the cell near the top electrode, helping better collection of photogenerated carriers at the electrode. Also, even when there was diffusion of Cu, thermal diffusion of excess indium at the top may help in the formation of a layer of In_2S_3 free of Cu at the top. Cell parameters obtained were V_{oc} = 533 mV, J_{sc} = 17.4 mA/cm^2, FF = 28.6% and η = 2.65% [Fig. 8.1].

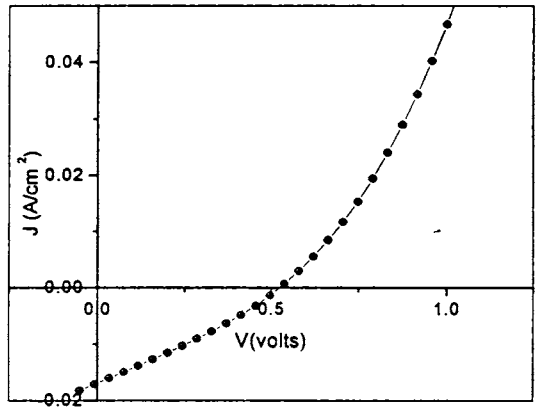

Fig. 8.1 J-V characteristics of Cell-A

XPS analysis of the cell [Fig.7.7] (before diffusing Indium) revealed diffusion of Cu from $CuInS_2$ layer to In_2S_3 layer. Copper diffusion is an easy process as the diffusion coefficient of Cu is high [6]. Moreover oxygen was present throughout the depth of the In_2S_3 layer when sprayed over $CuInS_2$, while there was no oxygen when In_2S_3 was sprayed alone [5]. This might have resulted in an increase of the resistance of the cell reducing FF.

8.3.2 Cell-B

The performance of the cell was improved by depositing two layers of $CuInS_2$ (as described earlier) and a single layer of In_2S_3. This time silver was deposited as the top electrode using vacuum evaporation. The area of electrode was 0.014 cm^2 and thickness ~ 45 nm. Fig. 8.2 shows the depth profile of the cell.

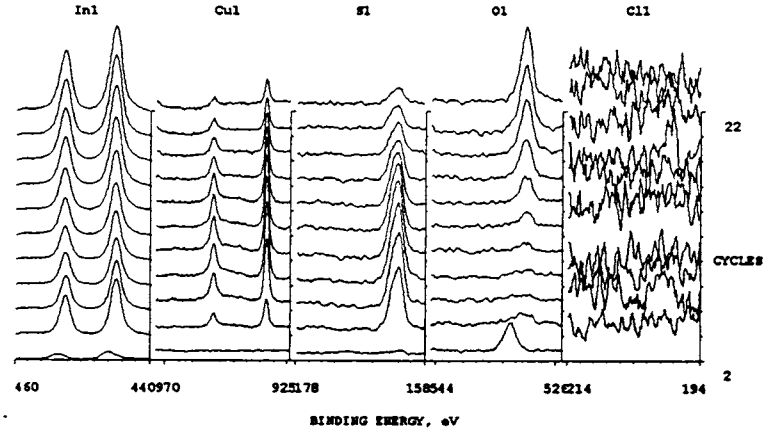

Fig. 8.2 XPS depth profile of Cell-B

Interestingly here it was clear from the XPS depth profile that there was no oxygen in the bulk of the sample when fabricated in three layers. This was not the case for the Cell-A having single layer of $CuInS_2$. This might be reducing resistance of the sample allowing better carrier collection at the electrode. However there was a peak at the surface of the cell, corresponding to binding energy 532.5 eV, representing presence of oxygen as surface contaminant. This was not doing any damage to the cell. Interestingly no peak corresponding to chlorine was present in the XPS results eventhough we used precursor solution containing chloride, for sample preparation. But when In_2S_3 layer was prepared, chlorine was present in it. Increase in the thickness of the absorber layer should increase the light absorption and hence the generation of photocarriers. Moreover concentration of Cu decreased towards the CIS/In_2S_3 interface as evident from peak height of binding energy of Cu in Fig.8.2. This probably made CIS layer near interface, more photosensitive. But still there was Cu diffusion as it was evident from the thin layer of In_2S_3 present over $CuInS_2$. Cell

parameters obtained in this case were V_{oc} = 450 m V, J_{sc} = 44.03 mA/cm^2, FF = 29.5 % and η = 5.87 %. The dark and illuminated J-V characteristics of the cell are given in Fig 8.3 and 8.4.

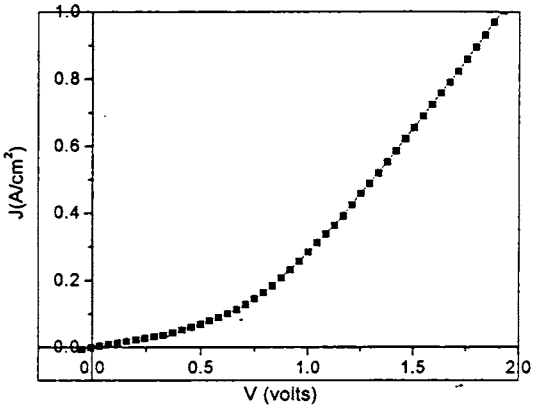

Fig. 8.3 Dark characteristics of Cell-B

Series resistance (R_s) calculated from the inverse slope of the dark forward characteristics of the cell was 1.23 Ω. The value can also be calculated from the equation

$$R_s = \frac{1}{\lambda}\frac{1}{(I_2 - I_1)}\ln\left[\frac{I_{ph} - I_2}{I_{ph} - I_1}\right] - \left(\frac{V_2 - V_1}{I_2 - I_1}\right)$$

where, λ = q/AkT; A is diode quality factor, kT/q is thermal voltage, I_{ph} is the light generated current density, V_1,V_2, I_1 & I_2 are the voltage and current density values at any two points on the J-V characteristic curve [7]. Series resistance was found to be 1.16 Ω. This was in good agreement with the value obtained from the dark forward characteristics of the cell.

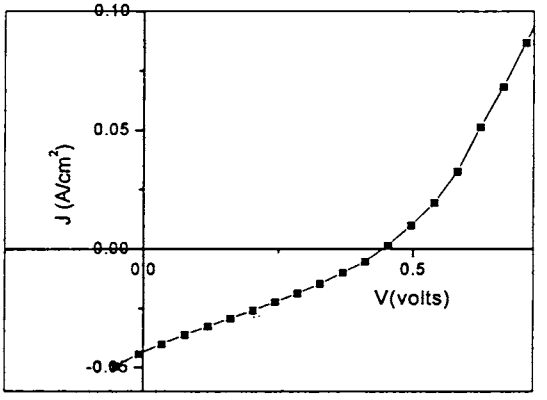

Fig.8.4 Illuminated J-V characteristics Cell-B

Diode quality factor calculated from the slope of the dark characteristics of the cell, by plotting ln (J) vs V graph was 2.5 [Fig. 8.5]. Therefore, forward dark J-V characteristics are dominated by the recombination-generation mechanism [8].

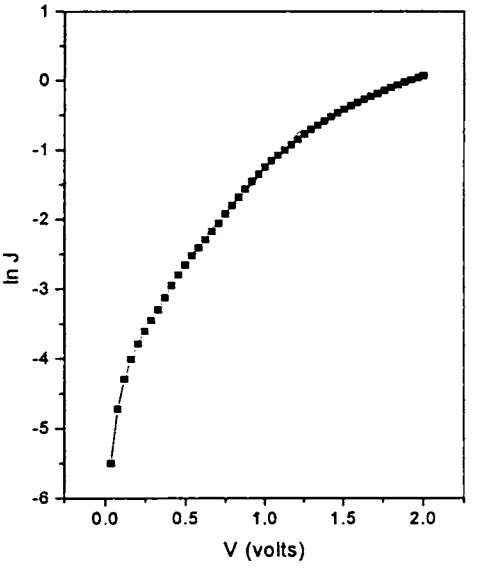

Fig. 8.5 ln J vs V graph (Cell-B)

Figure 8.6 shows results of XRD analysis of absorber and buffer layers of Cell-B. Both $CuInS_2$ and In_2S_3 phases are observed in the XRD results of the cell. In the absorption spectrum of the cell, the band edges corresponding to both the $CuInS_2$ and In_2S_3 layers were clearly observed [Fig.8.7].

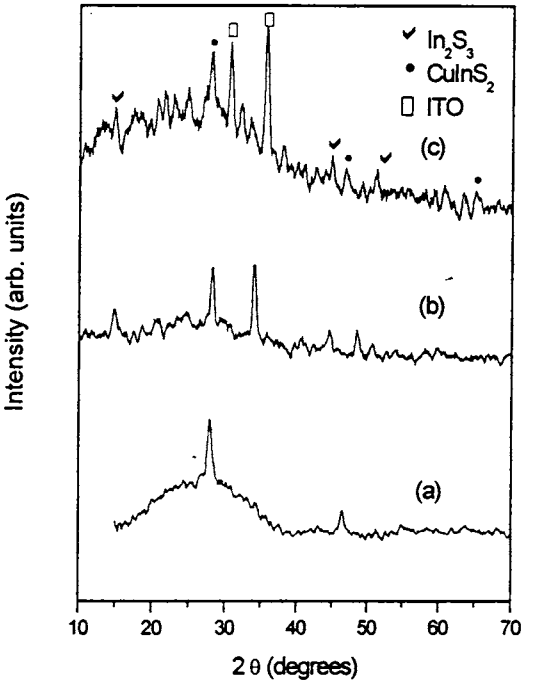

Fig. 8.6 XRD spectra of (a) $CuInS_2$ (b) In_2S_3 (c) ITO/$CuInS_2$/In_2S_3

Fig. 8.8 shows the spectral photoresponse of Cell-B. Cutoff at the short wavelength side was due to absorption in the In_2S_3 layer, while the long-wavelength cutoff corresponds to absorption edge of $CuInS_2$ film. Due to the higher band gap of Cd-free buffer layer, an enhanced response in the short wavelength region of the spectrum can be observed resulting in higher short circuit current. Collection property of this junction was sufficient as evident from the flatness of the spectral response.

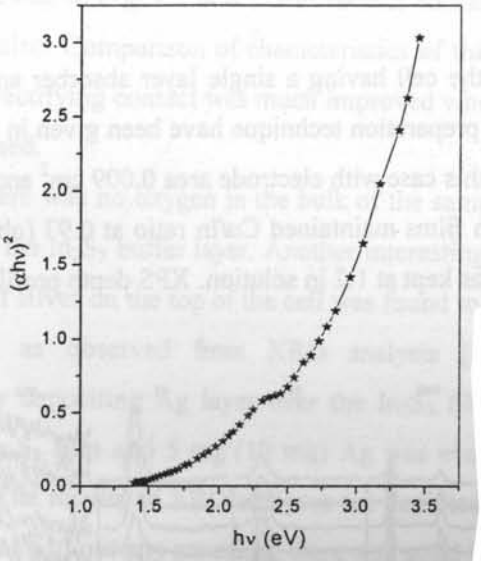

Fig. 8.7 $(\alpha h\nu)^2$ vs hν plot for Cell-B

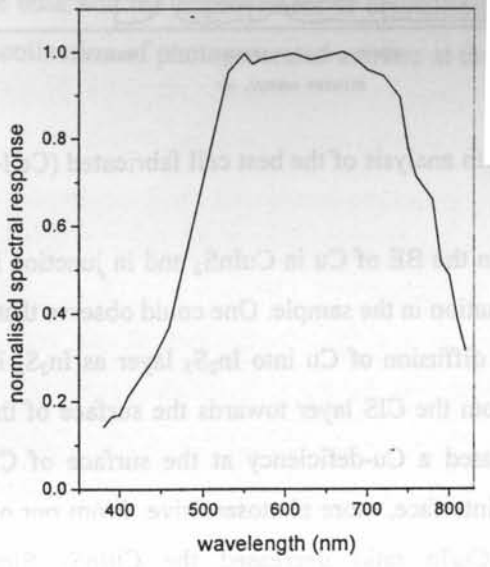

Fig. 8.8 Spectral response of Cell-B

8.3.3 Cell-C

Here we prepared the cell having a single layer absorber and a double layer of buffer layer. Details of preparation technique have been given in section 8.2. The top electrode was silver in this case with electrode area 0.009 cm^2 and thickness ~ 45 nm. In this case $CuInS_2$ thin films maintained Cu/In ratio at 0.93 (observed from EDAX analysis), as the ratio was kept at 1.2 in solution. XPS depth profile of the cell is given in Fig.8.9.

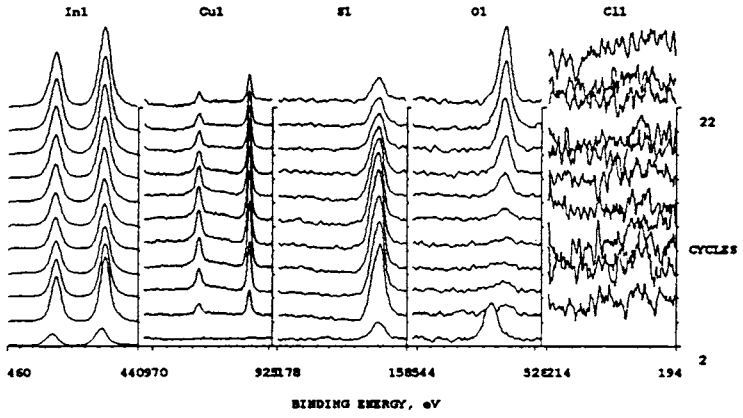

Fig. 8.9 Depth analysis of the best cell fabricated (Cell-C)

There was no shift in the BE of Cu in $CuInS_2$ and in junction indicating absence of any binary phase formation in the sample. One could observe that at the interface of $CuInS_2/In_2S_3$, there was diffusion of Cu into In_2S_3 layer as In_2S_3 is thin. Thus there was a gradient of Cu from the CIS layer towards the surface of the In_2S_3 film. This diffusion of copper created a Cu-deficiency at the surface of CIS layer probably making CIS layer, near interface, more photosensitive. From our own experience we had seen that when Cu/In ratio decreased the $CuInS_2$ films become more photosensitive [9]. However in the case of Cell-C one could see that there was a layer of In_2S_3 at the surface [Fig. 8.9] without any Cu. This layer of In_2S_3 was thicker than

such layers indicated in Fig. 7.7 & 8.2. But surface contamination due to oxygen was there in Cell-C also. Comparison of characteristics of this junction with earlier ones proved that the rectifying contact was much improved when the thickness of the In_2S_3 layer was increased.

Here also there was no oxygen in the bulk of the sample. This might be reducing the resistance of the In_2S_3 buffer layer. Another interesting point to be noted here was that deposition of silver on the top of the cell was found to improve the crystallinity of the In_2S_3 layer as observed from XRD analysis [Fig.8.10]. This was done independently by depositing Ag layer over the In_2S_3 film. 200 ml of solution was sprayed to get In_2S_3 film and 5 mg (10 mg) Ag was evaporated to deposit Ag film over In_2S_3 film. The results of XRD analyses are depicted in Fig. 8.10 (a) and (b). It was very clear that without any annealing there was good improvement in crystallinity of In_2S_3 sample (scale on Y-axis is the same for Fig. 8.10 (a), (b) and (c)). This might have resulted in considerable decrease in dark resistivity of In_2S_3. Hence the absence of oxygen in the bulk and the improvement of crystallinity of In_2S_3 might be helping to have a better collection of photogenerated carriers at the electrode.

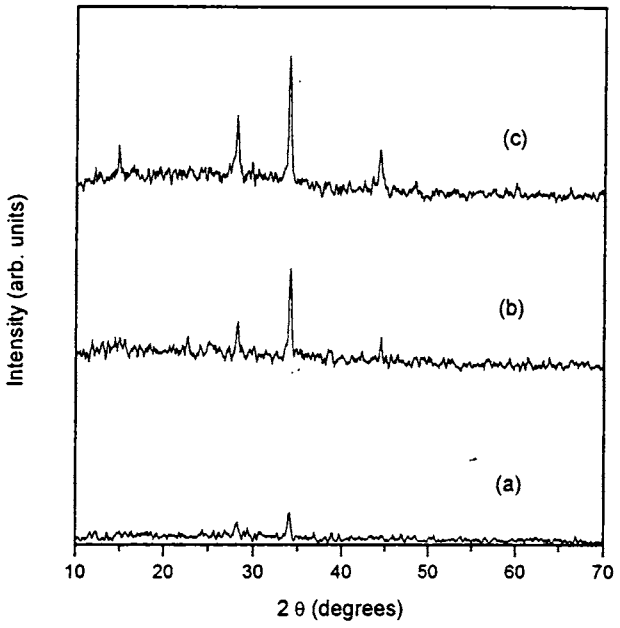

Fig. 8.10 XRD spectrum of In_2S_3 buffer layer (a) as prepared (b) coated with 5 mg Ag (c) coated with 10 mg Ag (without any annealing)

Dark and illuminated J-V characteristics of the cell fabricated in three layers is given in Fig.8.11. The cell parameters obtained were V_{oc} = 588 mV, J_{sc} = 48.2 mA/cm^2. FF = 33.5% and η = 9.5%. To the best of our knowledge this is the maximum efficiency obtained so far for a $CuInS_2/In_2S_3$ cell fabricated using CSP technique. On increasing Cu/In ratio conductivity of the $CuInS_2$ film increased, compared to the previous cases. This enhancement of conductivity of $CuInS_2$ films might be another reason for the increase in the value of V_{oc}, J_{sc} and FF [10].

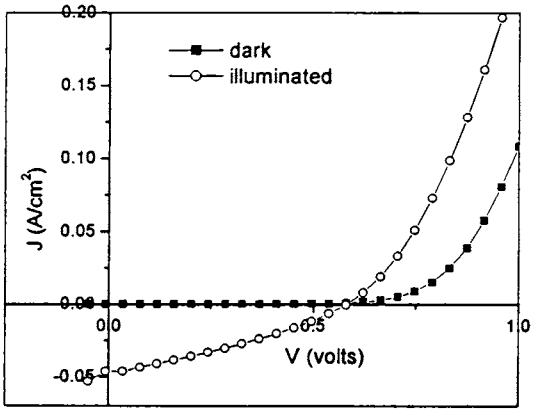

Fig. 8.11 Dark and illuminated J-V characteristics of the best cell fabricated (Cell-C)

We could find a violation of the superposition of light and dark characteristics, which is known as *cross over*; a phenomenon commonly encountered in CIS devices. Several publications [11-13] related this shift to the deep level acceptor states, which were present in the buffer layer or at the interface. In the present case also there could be deep level acceptors (like vacancy of In) in buffer layer as we kept In/S ratio equal to 1.2/8 to make indium low and sulfur excess as this resulted in high photosensitivity.

Series resistance (R_s) calculated from the inverse slope of the dark forward characteristics of the cell was 0.83 Ω. The value was found to be much less than that of Cell-A (14.2 Ω) and Cell-B (1.23 Ω). The J-V characteristics follow the general relationship J ~ exp (qV/nKT). Thus diode quality factor was calculated from the slope of the dark characteristics of the cell, by plotting ln (J) vs V graph. The value was found to be 2.2. Diode quality factor, greater than two, indicated the domination of generation - recombination process [14]. The interface recombination might be responsible for a moderate open circuit voltage and fill factor [15]. Absorption

spectrum of the cell was recorded in the wavelength range 350-950 nm. It showed clear absorption edges for both the absorber and buffer layers [Fig.8.12].

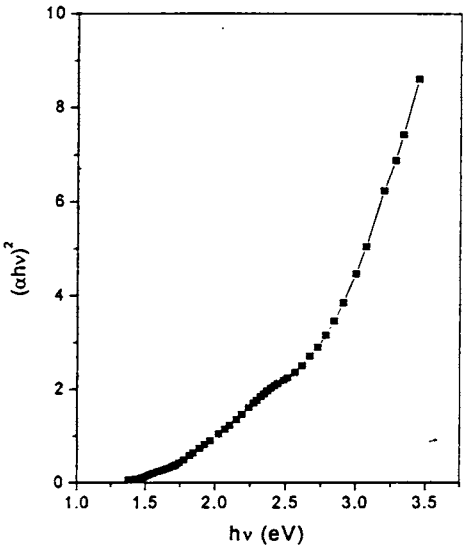

Fig. 8.12 Absorption edges for $CuInS_2$ and In_2S_3 (Cell-C)

Fig. 8.13 shows the normalized spectral response of the cell. The cutoff at short wavelength side was due to absorption in the In_2S_3 layer, while the long-wavelength cutoff corresponds to the absorption edge of $CuInS_2$ film. Due to the higher band gap of Cd-free buffer layer, an enhanced response in the short wavelength region of the spectrum can be observed resulting in a higher short circuit current. The overall response was flat indicating a sufficiently large collection width, ie, space charge region plus diffusion length [15].

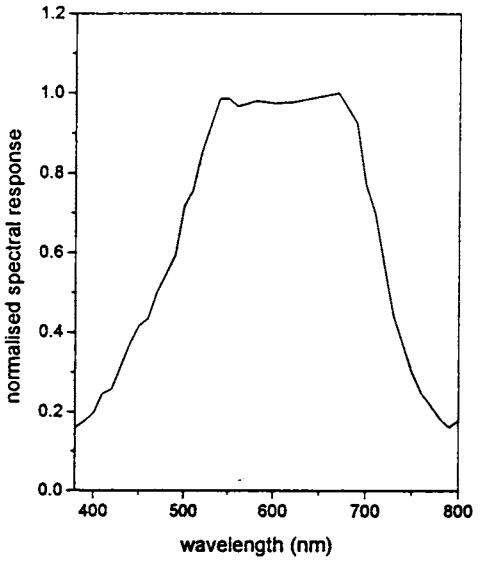

Fig. 8.13 Normalised spectral response of Cell-C

8.4 Conclusion

Cell fabricated with single layer of $CuInS_2$ and double layer of In_2S_3 (Cell-C) using CSP technique with Ag electrode (area 0.009 cm^2) exhibited 9.5% efficiency. This is the highest efficiency ever reported for $CuInS_2/In_2S_3$ cell fabricated using CSP technique. We found that there was diffusion of copper from the $CuInS_2$ layer to the In_2S_3 layer from XPS analysis. Absence of oxygen in the bulk of the sample and the presence of a layer of In_2S_3 free of Cu at the top of the cell might be contributing to the improvement in the performance of the cell when fabricated in three layers. A layer of silver coated on the surface of the In_2S_3 buffer layer helped in improving the crystallinity of the In_2S_3 layer as observed from XRD analysis. This might be resulting in better collection of photogenerated carriers at the electrode. All these might have contributed to the high efficiency of the cell.

References

[1] Y. Ogawa, A. Jäger-Waldau, Y. Hashimoto and K. Ito *Jpn. J. Appl. Phys.* **33** (1994) L1775

[2] T. Negami, Y. Hashimoto, M. Nishitani and T. Wada *Sol. Energy Mater. Sol. Cells* **49** (1997) 343

[3] J. Klaer, J. Bruns, R. Henninger, K. Siemer, R. Klenk, K. Ellmer and D. Bräunig *Semicond. Sci. Technol.***13** (1998) 1456

[4] T. Watanabe, H. Nakazawa, M. Matsui, H. Ohbo and T. Nakada *Sol. Energy Mater.Sol. Cells* **49** (1997) 357

[5] Teny Theresa John, S. Bini, Y. Kashiwaba, T. Abe, Y. Yasuhiro, C. Sudha Kartha and K. P. Vijayakumar *Semicond. Sci. Technol.* **18** (2003) 491

[6] K. Djessas, S. Yapi, G. Massé, M. Ibannain and J. L. Gauffier *J. Appl. Phys.* **95 (8)** (2004) 4111

[7] M. K. El-Adawi and I. A. Al-Nuaim *Vacuum* **64** (2001) 33

[8] L. L. Kazmerski and G. A. Sanborn *J. Appl. Phys.* **48(7)** (1977) 3178

[9] Teny Theresa John, K. C. Wilson, P. M. Ratheesh Kumar, C. Sudha Kartha, K. P. Vijayakumar, Y. Kashiwaba, T. Abe and Y. Yasuhiro *Phys. Stat. Sol. (a)* **202 (1)** (2005) 79

[10] R. Scheer, M. Alt, I. Luck and H. J. Lewerenz *Sol. Energy Mater. Sol. Cells* **49** (1997) 423

[11] M. Igalson and C. Platzer-Björkman *Sol. Energy Mater. Sol. Cells* **84** (2004) 93

[12] M. Gloeckler, C. R. Jenkins and J. R. Sites *Proc. Mat. Res. Soc. Symp.* **763** (2003) B5.20.1

[13] I. L. Eisgruber, J. E. Granata, J. R. Sites, J. Hou and J. Kessler *Sol. Energy Mater. Sol. Cells* **53** (1998) 367

[14] L. L. Kazmerski, F. R. White, M. S. Ayyagari, Y. J. Juang and R. P. Patterson *J. Vac. Sci. Technol.* **14(1)** (1977) 65

[15] T. Walter, A. Content, K. O. Velthaus and H. W. Schock *Sol. Energy Mater. Sol. Cells* **26** (1992) 357